Nuclear Magnetic Resonance Spectroscopy in Solid Polymer Electrolytes

W. Gorecki
Laboratoire de Spectrométrie Physique, Université Joseph Fourier
B.P. 87 - 38402 Saint-Martin-d'Hères - France

P. Donoso
Instituto de Física e Química, Universidade de São Paulo
Caixa Postal 369, São Carlos, 13560-970, SP, Brasil

M. Armand
Laboratoire d'Ionique et d'Electrochimie du Solide, Institut National Polytechnique de Grenoble
B.P. 75 - 38402 Saint-Martin-d'Hères - France

Received June 16, 1992

We present a review of Nuclear Magnetic Resonance (NMR) investigations of the complexes formed between alkali metal salts and Poly(ethylene oxide). We outline the salient features of such new class of ionic conductors as seen through NMR techniques. The first section deals with structural information, ie, phase diagrams and determination of internuclear distances. The second section contains dynamical information, ie, their conducting mechanism, the influence of the glass temperature and the determination of diffusion coefficient and transport numbers. Dominant relaxation mechanisms and fundamental interactions are identified.

I. Introduction

The domination "polymer electrolytes" covers a variety of materials which show ionic motion in the solid-state. The simplest representatives are obtained by dissolution of a metalic salt in a solvating polymer. Several reviews and monographs[1,17,29] have been devoted to the subject with the motivation to elucidate the conduction mechanism and to use them for applications in the important domains of high energy density batteries, electrochromic systems, photoelectrochemical cells and sensors. The power of magnetic resonance methods to study the dynamics of ionic conductors on the microscopic level has been recently reviewed[13,17].

Our aim in the present article is to present an overview of Nuclear Magnetic Resonance (NMR) Spectroscopy as a powerful technique for investigations in poly(ethylene oxide) - PEO:salt complexes.

Some general considerations can be sumarized:

1) polyethers like poly(ethylene oxide) -PEO- have solvating properties towards cations which are comparable to those of water, but they do not provide for anion solvation. Salts which form complexes with polymers are those with large delocalized negative charges, like I^-, ClO_4^-, $CF_3SO_3^-$; such anions do not require extensive H-bond type stabilization. Likewise, most studies have been made with alkali metal ions, especially lithium, considering its pivotal role in intercalation solid-state reactions. Inorganic acids (H_3PO_4, H_2SO_4...) also form complexes with polyethers and polyamines and display high proton conductivity.
2) stereoregular polymers, again like PEO, are semicrystalline materials coiled into a regular helical structure at temperature below the lamellae melting point of 65°C. A similar helical structure has been demonstrated by Chatani and Okamura[2] for the stoichiometric complex $P(EO)NaI_{1/3}$, as shown in Fig. (1). Either Li or Na derivatives behave similarly, obeying a phase diagram where the stoichiometric complexes, $x^{-1} = 3$ or 6 form an eutectic with pristine PEO. Above the liquidus line, the polymer-salt adducts are amporphous elastomers (Fig. 2).

Nuclear magnetic resonance is a powerful tool for studying solid polymer electrolytes, as it provides two kinds of informations:

- structural informations, like the phase diagram

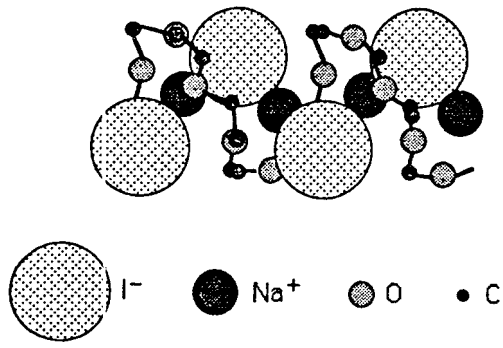

Figure 1.: The helical structure of $PEO(NaI)_{1/3}$, as determined by X ray crystallography. From ref. [2].

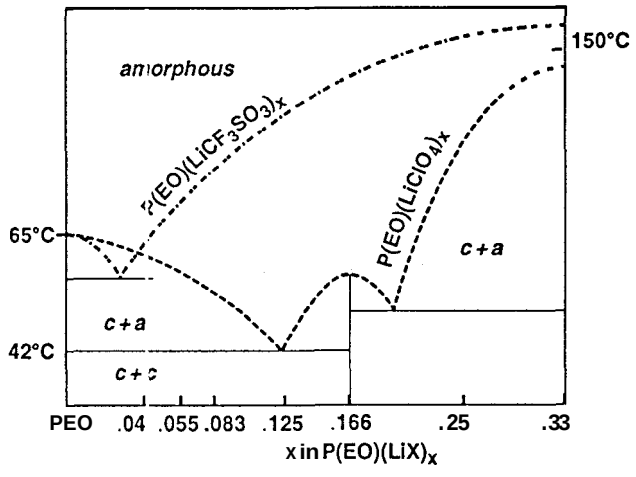

Figure 2.: Examples of phase diagrams in the PEO-LiX systems ($X = ClO_4^-, CF_3SO_3^-$). c = crystalline; a = amorphous.

which is difficult to establish due to a considerable tendency for supercooling. The determination of the relative fraction of protons belonging to the polymer chain and of cations and anions which are in the crystalline phase, in the case of semicrystalline polymer, provides the necessary information. The internuclear distances between various nuclei can be determined by analyzing the line shape of the resonance lines (theory of moments)

dynamical informations. The knowledge for various nuclei of the longitudinal or spin-lattice relaxation time T_1 versus the frequency allows the determination of the correlation time τ_c of the diffusional processes. The comparison of τ_c with conductivity data is a good test to assert that the ionic conductivity is goveriied by the segmental motion of the chains. However, the frequency dependenie of $T_{1\rho}$ and T_1 (relaxation time in the rotating and laboratory frame) is difficult to interpret beeause these data strongly depart from the classical BPP (Bloembergen, Purcell and Pound) model[6,12].

Finally, the determination of the anionic and cationic diffusion coefficients can be perforined by the pulsed magnetic field gradient technique (PMFG) which provides informations about the transport numbers t^+ and t^-.

II. Structural Informations

II.1 Determination of the phase diagram

For a good understanding of the dynamic of the microscopic mechanisms which are implicated in the motions of the anions and cations, it is essential to determine the phase diagram of semicrystalline polymers such as $P(EO)(LiCF_3SO_3)_x$, P(EO) $(NaI)_x$ and $P(EO)(LiClO_4)_x$ [3,5–7]. From NMR experiments we can obtain the respective amounts of crystalline and amorphous phases and the salt concentration in both phases. In section II, we shall show how to determine the nature of the conducting phase.

The technique used is pulsed NMR at the Larmor frequency v = 22 MHz. NMR methods offer a particular advantage because in a given run, a specific nuclear species can be selected. We therefore observe the decrease of the transverse nuclei magnetization M_x. The transverse nuclei magnetization correlation function $G(t) =< M_x(t)M_x(0) >$ was determined by combining free induction decay and spin-echo techniques in order to cover a $6.10^{-6} - 10^{-1}$s observation range. For such measurements, the recovery time of the NMR receiver was $6\mu s$. In the semicrystalline state, $G(t)$ can be written as: $G(t) = G_1(t)+G_2(t)$, where $G_1(t)$ and $G_2(t)$ stand for the contribution of nuclei in the crystalline (or vitreous) and elastomeric phases respectively. Provided that the observed nuclei in the crystalline phase are not too far above the motional narrowing conditions and that the spin-lattice relaxation time in the elastomeric phase is not too short, $G_1(t)$ and $G_2(t)$ decay with very different time scales; this allows to separate the relative amount of nuclei belonging to the different phases from the ratio:

$$G_i(0) \,/\, G(0) \;=\; N_i \sum_i N_i, \qquad (1)$$

where N_i is the number of nuclei belonging to the i pliase. This procedure was applied, for example, to determine the fractions of protons $^1C = {}^1G_c(0)/{}^1G(0)$ and the fractions of lithiums $^7C = {}^7G_c(0)/{}^7G(0)$ in the crystalline phase in the compound $P(EO)(LiClO_4)_{0.285}$ (Figure 3). If x denotes the number of cations per monomer unit in the complex and x_c the number of cations per monomer unit in the crystalline phase, it is easy to show that $x_c = x\,{}^7C/{}^1C$. In our example of figure 3, we find $x_c = 0{,}285$ at T = 84°C.

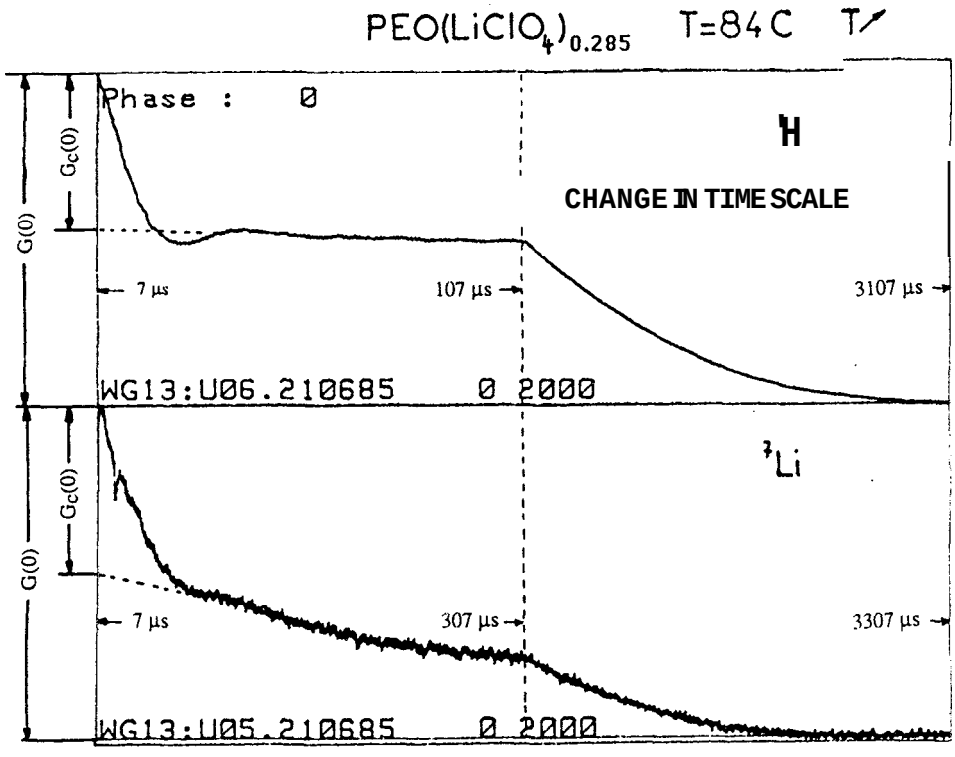

Figure 3.: Decrease of the transverse magnetization with time of the protons and lithiums in semicrystalline complex P(EO) $(LiClO_4)_{0.285}$ at $T = 84$ C.

This procedure can be applied to determine, at each temperature, the stoichiometry of the crystalline and elastomeric (amorphous) phases. In Figure 4, we show the fractions of protons ^1C and fluorines ^{19}C belonging to the crystalline phase in P(EO) $(LiCF_3SO_3)_{0.125}$. The striking result is the absence of variation of ^{19}C until **328** K, whereas the fraction of protons ^1C starts to decrease from room temperature. This clearly demonstrates that the sharp drop in the crystallinity at the transition temperature is due to the melting of uncomplexed P(EO) and thus the crystalline phase left above that temperature is a salt-rich complex of PEO which progressively dissolves in the elastomeric phase. The temperature **T = 328** K coincides well with the change of slope of the ionic conductivity vs. temperature as shown in Figure 5. We have represented in Figure 6 the equilibrium phase diagram deduced from NMR measureinents between uncomplexed P(EO), P(EO) $(LiCF_3SO_3)_x$, with $10 < x^{-1} < 4$ and the amorphous phase (for more details see ref. 3,4). These results are corroborated by differential scanning calorimetry measurements.

11.2. Determination of the internuclear distaiices

The second moment (M_2) of a resonance curve, i.e., its normalized moment of inertia about the central axis of symmetry, is proportional to the inverse sixth power of the distances between the resonating nuclei (homonuclear contribution) and all other nuclei with nonzero magnetic moment (heteronuclear contribution)[6]. Thus, the moment is a measure of the nuclear interactions. As a practical consequence of the inverse-sixth-power decay, only nearest and next-nearest neighbours make appreciable contributions.

This parameter of the NMR line shape measured at adequately low temperatures, i.e., in the rigid-lattice regime, has been extensively evaluated for structural investigations of molecular-solid crystals[6,9]. As the temperature rises out of that regime, the characteristic frequency of the molecular motion - the nuclei can move over considerable distances - grows, approaching the natural width of the resonance. The NMR line consequently narrows. The value of the temperature-dependent second moment typically drops sharply at a well-defined temperature, falling from a relatively high rigid-lattice plateau $(M_2 > 1G^2)$ to a very low, motionally narrowed limit $(M_2 < 1G^2)$.

In a crystalline phase, the free induction decay (FID) of nuclei is approximatively gaussian. By Fourier transform we obtain a gaussian NMR line shape. For dipolar interactions between protons in pure P(EO), the second line moment is given by[6] :

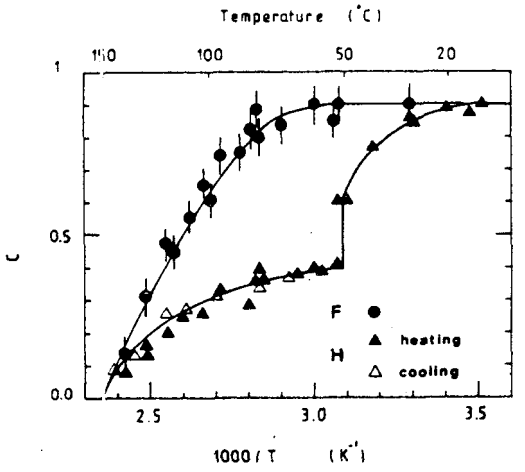

Figure 4.: Fractions of protons and ^{1}C (A, A) and fluorines ^{19}C (•) belonging to the crystalline phase in P(EO) $(LiCF_3SO_3)_{0.125}$, as a function of temperature. The sharp drop in ^{1}C at 326 K is due to the melting of uncomplexed PEO.

$$M_2 = \frac{3}{5}\gamma^4\hbar^2 I(I+1)\sum_k \frac{1}{r_{jk}^6}, \qquad (2)$$

where r_{jk} are the distance between interacting spins, 7 is the gyromagnetic ratio and I the nuclear spin. In this equatior , we assume an isotropic orientation of the crystallites.

Experimentally, we found $M_2^{H-H} = 14G^2$ for the four equivalrnt PEO protons in the monomer unit $(-CH_2 - CH_2 - O-)$. The nearest neighbor contribution would lead to a H − H distance (of the CH_2 group) of 1.72 Å, to be compared with the crystallographic determination H − H = 1.78 Å [7]. Let us stress that the next nearest neighbor contribution has a negligible contribution to the second rnoment (≈ 6%). An extensive study of the second moment of the proton, lithium and fluosine has been made in the compounds P(EO) $(LiBF_4)_x$, P(EO) $(LiA_sF_6)_x$ and P(EO) $(LiCF_3SO_3)_x$ [8]. The results are listed in Table I.

Let us ncw focus our attention on the ion-polymer and the ion-ion interactions. The proton second moments for litliium-salt complexed PEO and for uncomplexed PEO are different. It can be therefore concluded that the polymer chain volume changes after complexation.

The most remarkable feature of these data is the reduced seconc moments for fluorine. The experimental moments are significantly lower than any of those ones calculated for the groups BF_4 and AsF_6 [9]. A model explaining the small fluorine second moment considers the rotational reorientation of the BF_4 and AsF_6 ions: all nearest neighbour F-F pairs interchange their position for a shcrt time. In this model, the intramolecular

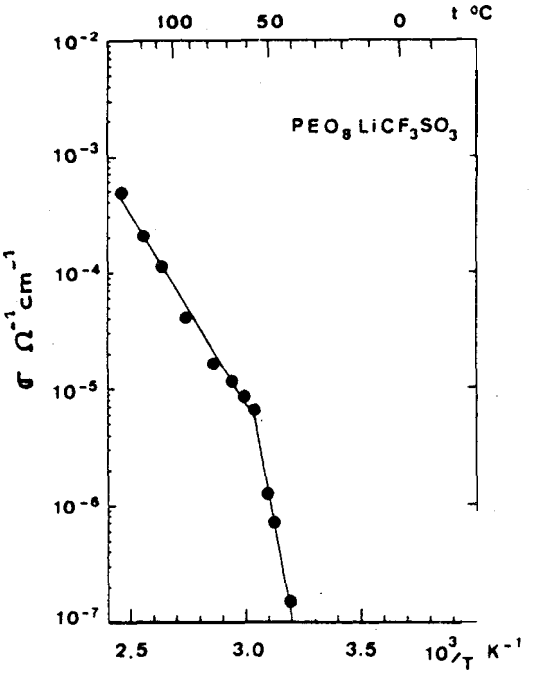

Figure 5.: Ionic conductivity versus the inverse temperaure during a cooling process in P(EO) $(LiCF_3SO_3)_{0.125}$.

second moment contribution is averaged to nearly zero, and the only narrowing mechanism available to explain the ^{19}F resonance line is due to residual interionic or intramolecular F-H and F-Li contribution. As proposed by Miller and Gutowsky in their NMR study of solid alkali hexa-fluorophosphates[10], a restricted rotational model may be also postulated to explain the reduction of second moments. For the P(EO) $LiBF_4$ complex, the ^{7}Li second moment comprises the following contributions:

$$M_2(Li) = M_2(Li-\mathrm{Li}) + M_2(Li-\mathrm{H}) + M_2(Li-\mathrm{B}) + M_2(Li-\mathrm{F}), \qquad (3)$$

In order to discriminate among these three contributions, we have used the NMR decoupling method. The heteronuclear-decoupling double-resonance technique simplifies the complex NMR spectra of nuclei by removing specific direct dipolar interactions between nuclei and decoupling the offending spins of interest. Such a removal is achieved with a second RF (radio frequency) field with frequency in the range of the Larmour frequency of the coupled nuclei[15]. For the polymer complexes here investigated, it has been concluded that at 230 K, the Li-H interaction seerns to be the dominant contribution to explain the observed lithium linewidth. The Li-F interaction, when present, is second in importance.

A similar study was made by Wintersgill et al[11] in order to determine the internuclear distance Li-Li in poly(vinyl acetate)$(LiClO_4)_x$ by analyzing the

Table I: Second moments (in Gauss^2), for PEO and various $P(EO)_nLiX$ complexes with n = 6 or 8, at 253 K. For comparison, the fluorine second moments of polypyrrole: BF_4 and in solid $LiBF_4$ are also shown[9].

	H	Li	F
PEO	14 ± 0.6 (290) K		
POE:$LiClO_4$	-	$1.6 \pm 0.2 (n = 6)$ $2.7 \pm 0.3 (n = 8)$	-
POE:$LiBF_4$	11.8 ± 0.5	5.8 ± 0.6 (fast component)	1.8 ± 0.1 theor: 14.3
POE:$LiAsF_6$	13.2 ± 0.5	5.5 ± 0.2 (fast component)	1.2 ± 0.1 theor: 12.2
POE:$LiCF_3SO_3$	18.0 ± 1.1		1.9 ± 0.1
PPy:BF_4	-	-	16 ± 2 (low T) 1.7 (high T)
$LiBF_4$	-	-	23.5 (low T) 2.7 (high T)

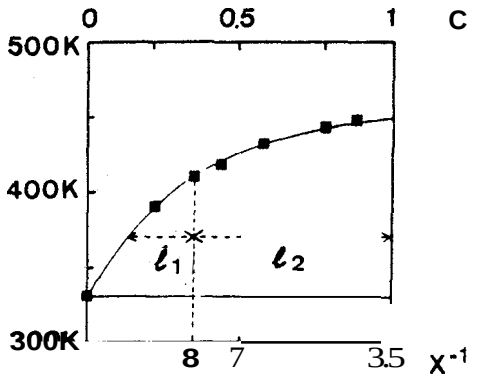

Figure 6.: Equilibrium phase diagram between uncomplexed P(EO), $P(EO)(LiF_3SO_3)_{0.285}$ and the elastomeric phase deduced from NMR experiments. Since the stoichiometry of the salt rich crystalline complex is x = 1/3.5, c = 3.5 x denotes the concentration of the complex, where c = 0 and 1 corresponds to pure PEO and pure $PEO(LiCF_3SO_3)_{0.285}$, respectively. The figure illustrates the crystallinity determination of the complex $x^{-1} = 8$ at 370 K, given by $^1C = l_1/l_2 + 12$.

linewidth of the lithiums. They conclude that $d_{Li-Li} \approx$ 4.5 A.

III. Dynamical Informations

A decade ago, the problem of the conduction mechanisrns in semicrystalline polyethers alkali metal salts was far from being understood. Clues for an answer was given by NMR spectroscopy. By analyzing the linewidths of the lithiums and fluorines in $P(EO)(LiCF_3SO_3)_{0.25}$ [3] we have shown that no motional narrowing occurs for the ^7Li and ^{19}F resonance lines in the crystalline phase up to 360 K, (Figure 4), indicating that neither the cation nor the anion are mobile in this phase. Therefore, the ionic mobility is restricted to the elastomeric phase.

III.1. Conducting mechanisms

Let us consider a polymeric solid ionic conductor whose cations and anions diffuse rapidly at temperatures above T_g. The charged species have nonzero magnetic moment. When they diffuse (a transport process probably assisted by the segmenta1 motion of the polymer) the nuclear moment is subject to a time dependent, random magnetic field, which causes the nuclear magnetization to relax dynamically[6]. Specifically, the nuclear relaxation results from the modulation of the nuclear-spin dipole-dipole interactions by the ionic and molecular motions. For a system of spin-1/2 pairs in contact with a heat bath at temperature T and under a magnetic field $B = \omega/\gamma$, the spin-lattice relaxation rate has the form

$$T_1^{-1}(\omega, T) = AJ(\omega, T), \qquad (4)$$

where A, a measure of the dipole-dipole interaction, is determined by the structural geometry and the number of interacting nuclei. $J(\omega, T)$, a sum of spectral densities and depends on the Larmor frequency and on a series of parameters characterizing the motion.

However, if the mobile spin exceeds 1/2, as it is the case with ^7Li and ^{23}Na, its electric quadrupole moment will interacts with the electric field gradient due to the charge distribution in its vicinity. The quadrupole interaction is the source of strong relaxation; its contribution should be added to the right-hand side of the relaxation rate eq. (4) and the quadrupolar term is proportional to ν_Q^2, where ν_Q is the coupling constant. For PEO-$LiCF_3SO_3$, around room temperature, ν_Q at the lithium sites is in the order of 0.2 MHz [29].

In most cases, the relaxation rate will depend on temperature through an effective correlation time r, expressed by an Arrhenius law ($\tau = \tau_0 \exp E/kT$) or by a VTF (Vogel-Tamman-Fulcher) law [r = $\tau_0 \exp(\Delta E/k(T - T_0)]$, wliich introduces the activation energy E and the pseudoactivation energy AE, as well as the pre-exponential factor τ_0. In the simplest case of discrete, classical charge transport, the activation energies extracted from conductivity and NMR measurements should agree. The correlation time defines the time scale for changes of the local magnetic field experienced by tlie resonant nuclei. Crudely, it can be interpreted as the time between ionic hops between equivalent positions, i.e., the time that controls transport properties. To interpret physically the parameter τ_0^{-1} one can adopt a harmonic approximation for the periodic potential in which the ion moves. The attempt frequency τ_0^{-1} can then be interpreted as a vibrational frequency where value is of the order of an optical-phonon frequency ($10^{12} - 10^{13} s^{-1}$).

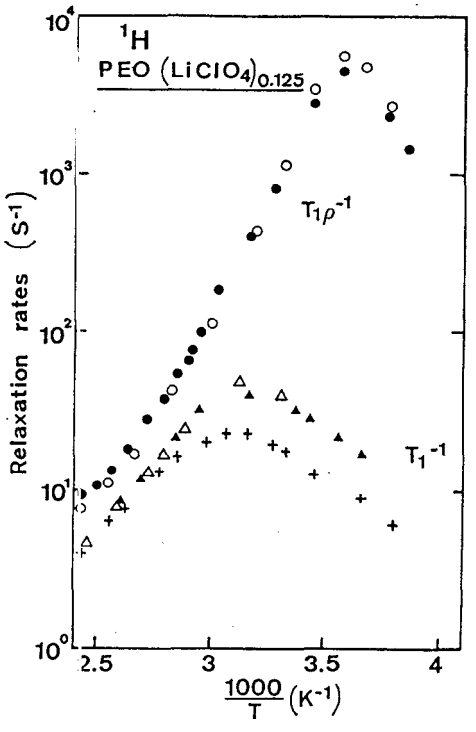

Figure 7.: Proton NMR relaxation rates as a function of reciprocal teinperature in P(EO) $(LiCl_4)_{0\,125}$. The values of $T_{1\rho}^{-1}$ a-e plotted for a Larmor frequency $\nu_0 = 19$ MHz (A cooling, ▲ heating) and $\nu_0 = 34$ MHz (+ cooling). The $T_{1\rho}^{-1}$ measurements were performed for the same frequencies (o $\nu_0 = 19$MHz, • $\nu_0 = 34$ MHz) in a cooling process and correspond to a rotating magnetic field $H_1 = 5$ Gauss.

The relaxation time in the laboratory frame, T_1, and in the rotating frame, $T_{1\rho}$, studied versus frequency and temperature, give an estiination of the correlation time r,. An elementary analysis of T_1^{-1} versus T^{-1} curves was presented by Bloembergen, Purcel and Pound (BPP)[12], who assumed random motion and dynamically equivalent environments for all ionic units. For a distribution of times between hops following a Poisson distribution the correlation function is a simple exponential and $1/T_1 = A_{\tau_c}/1 + \omega^2 \tau_c^2$ [6,14,15].

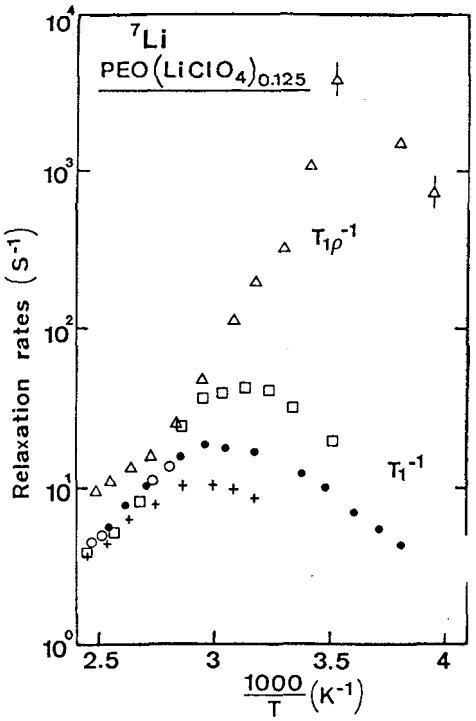

Figure 8.: Lithium NMR relaxation rates as a function of reciprocal temperature in P(EO) $(LiClO_4)_0$ 125. The values of T_1^{-1} are plotted for a Larmor frequency $\nu_0 = 8$MHz (□ cooling), $\nu_0 = 19$ MHz (o cooling, • heating) and $\nu_0 = 19$ MHz (+ cooling). The $T_{1\rho}^{-1}$ measurements were performed for $\nu_0 = 19$ MHz (A) in a cooling process and correspond to a rotating magnetic field $H_1 < 5$Gauss.

When the correlation time is thermally activated $\tau_c = \tau_0 \exp(-E/kT)$ and for a fixed Larmor frequency ω_L, $1/T_1$ presents a symmetric shape as a function of reciprocal absolute temperature and its maximum is given by the condition $\omega_L \tau_c = 1$. Deviations of the data from the BPP-type behavior are frequent[8,13]: i) in a plot log $\tau_c T_1$ versus the inverse temperature, the curve may not be symmetric with respect to the value where T_1 minimum occurs; ii) the activation energies E deduced from these slopes may not agree with those obtained from conventional diffusion measurements and especially from conductivity data. The main reason of this lack of agreement is that NMR explores the dynamics of the system at a molecular scale, whereas conductivity measurements display mainly macroscopic properties of the compound: the local motion of the nuclei is seen by NMR while only long range displacement cor-

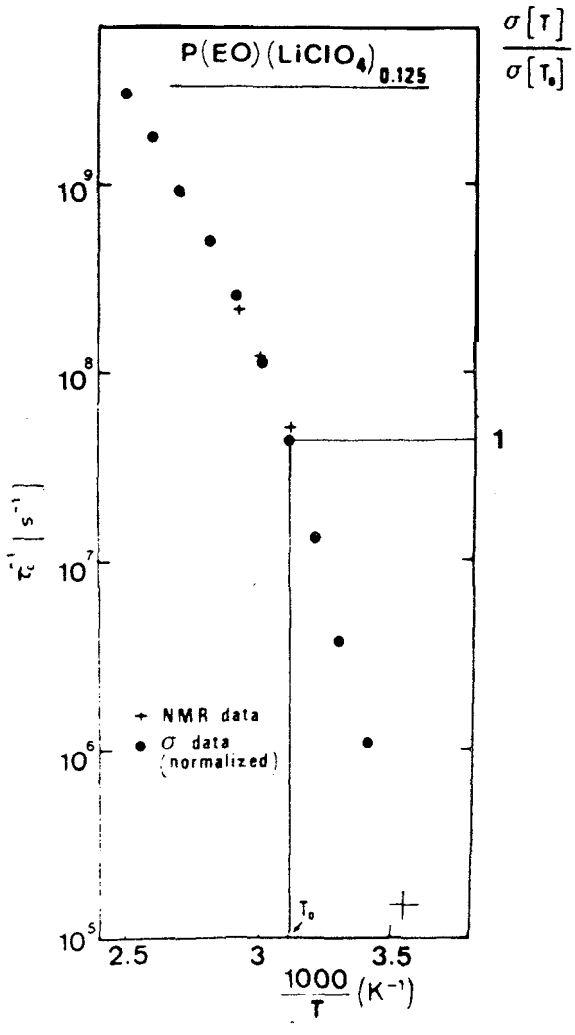

Figure 9.: Temperature dependence of the proton correlation time τ_c deduced from the maxima of the relaxation rates at various frequencies. On this figure, we have also plotted the conductivity $\sigma(T)/\sigma(T_0)$ with $T_0 = 333$ K versus $1/T_0$. For clarity sake, the point $\sigma(T_0)$ was taken identical to the point $\tau_c^{-1}(T_0)$.

responding to the effective charge transfer is needed for conductivity. NMR is also insensitive to the charge of the nuclei and reflects the mobility of neutral species (ion pairs). An especially detailed study of the complex P(EO) $(LiClO_4)_{0.125}$ has been performed. NMR relaxation rates of the various resonant nuclei involved in that compound were determined in the laboratory $(1/T_1)$ and in the rotating frame $(1/T_{1\rho})$ at various temperatures and for different frequencies, with the aim of comparing the microscopic behavior of the cations and of the protons in the polymer chains. We present in Figures 7 and 8, the femperature dependence of ^{1}H and ^{7}Li NMR relaxation rates in P(EO) $(LiClO_4)_{0.125}$ for $260K < T < 400$ K. It is apparent that there is no difference between the curves obtained through a cooling and a heating process. This means that no recrystallization takes place[5] and that the complexes are especially prone to supercooling at the eutectic composition $x^{-1} = 8$. Most striking is the similar behavior of the ^{1}H and ^{7}Li relaxation rates. Both rates peak at the same temperature and show the same frequency dependente. This implies that the relevant spectral densities involved in the relaxation of both species are essentially the sanie, i.e., that the random motion of cations is mainly governed by segmental motion of polymer chain.

As it has been shown above it is possible to derive the order of magnitude of the correlation times (at the minimum of T_1) for various temperatures. We have plotted in Figure 9 the values of τ_c^{-1} corresponding to the maximum of the ^{1}H proton relaxation rates, obtained from Figure 7, versus the inverse temperature for various resonance frequencies. As $1/T_{1\rho}$ presents also a maximum for $2\omega_L\tau_c = 2\gamma H_1\tau_c \approx 1$ [15], the corresponding point is also reported on the diagram. On the same figure, we have also plotted the relative thermal variation of the measured macroscopic conductivity of the complex. It is clear that τ_c^{-1} values scale fairly well with the conductivity data, within the limits of experimental errors. This shows unambiguously that the conductivity is governed by segmental motion of chains as previously observed in P(EO) $(H_3PO_4)_x$ [16].

A further theoretical analysis is required in order to understand why ^{7}Li and ^{1}H relaxation times have almost the same magnitude. It seems presently to be a simple coincidence.

For several amorphous polymers, it has been suggested that the correlation time τ_c should follow the Vogel-Tamman-Fulcher (VTF) relaxation law[17] given by $\tau_c = \tau_0 \exp B/T - T_0$ where B is often referred as a pseudoactivation energy and T_0 is the ideal glass transition temperature typically assumed to be equal to $T_g - 50$ K, where T_g is the glass transition temperature measured by differential scanning calorimetry. In our samples, however, no satisfactory fit could be obtained.

III.2. Distribution of correlation times

The source of discrepancy between the BPP model and much of the relaxation data is easily identified: in contrast with the fundamental assumption of Ref. 12, in many complex condensed-matter systems the relaxation processes are nonexponential with respect to time over many orders of magnitude around the Larmor frequency. Transport and relaxation in disordered solids such as amorphous polymers, molecular-solid solutions and glasses, involve microscopic processes possessing no characteristic time scale. Furthermore, transport of ions frequently takes place in less than three dimensions, which affects the correlation functions.

A simple extension of the BPP model assumes that the correlation function is a distribution of exponentials; in systerns where different environments are available to the mobile ion, this generalization seems reasonable. Various distributions derived from the Debye spectral density have been examined by Beckmann[33].

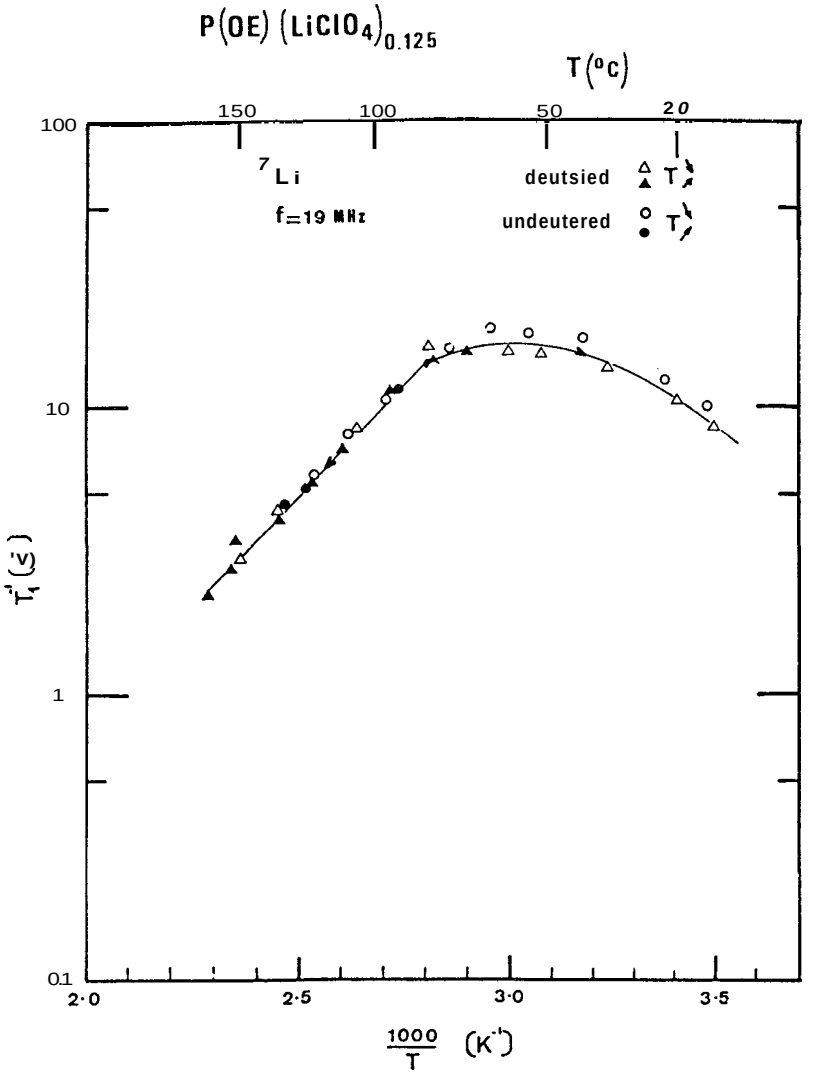

Figure 10.: Comparision between the relaxation rates $1/T_1$ of ^{7}Li nuclei in P(EO) $(LiClO_4)_{0.125}$ complex in the hydrogen compound (o) and in the fully deuterated compound (A) in a cooling process for $285 < T < 435$K. The resonance frequency was $\nu_0 = 19$ MHz.

Another convenient way to describe the relaxation processes in disordered systems is to use the so-called stretched exponential correlation function[19] or the William-Watts function[20], where $G(t) = \exp -(t/\tau)^\beta$ with $\beta < 1$ The William-Watts correlation function is interpreted in terms of a distribution of correlation times τ_c. It is often used to fit mechanical and dielectric relaxation ditta. In such a description, the spin-lattice relaxation time at low temperature, where $\gamma H_0 \tau >> 1$, has the form: $T_1 \approx (\gamma H_0)^{(1+\beta)} \tau^\beta$. Such a description was used to interpret the relaxation time T_1 of phosphorus in the protonic conducting $P(EO)(H_3PO_4)_x$, where the experimental data strongly depart from the BPP behavior[16].

An estimation of β was made from an implicit plot of σT which is proportional to $\tau_c^{-1}(T)$, and leads to $\beta = 0.27$. The T_1^{-1} temperature dependence is reproduced quite adequately and the frequency dependence of T_1 and $T_{1\sigma}$ is correct. However, it is difficult to extract microscopic informations concerning the ions diffusion from the β factor.

111.3. Relaxation mechanisms

^{1}H, ^{19}F and ^{7}Li spin-lattice relaxation investigations in Lithium-salt:PEO complexes allow us to understand the mechanism governing the proton, fluorine and lithium relaxation and to characterize the dynamics of the polymer chain of the cation (Li^+) and of the anion.

In order to investigate precisely the various relaxation mechanisms, proton relaxation rates $1/T_1$ have been measured in a compound where all ^{7}Li have been replaced by ^{6}Li isotope which has a lower gyromagnetic factor: $^6\gamma/^7\gamma \approx 2.6$. Similarly, ^{7}Li relaxation rates have been measured in deuterated compound. The results are shown in Figures 10 and 11. It is clear that isotopic substitution has practically no measurable effect. This shows that the magnetic dipolar interaction between lithium and hydrogen nuclei has no influence

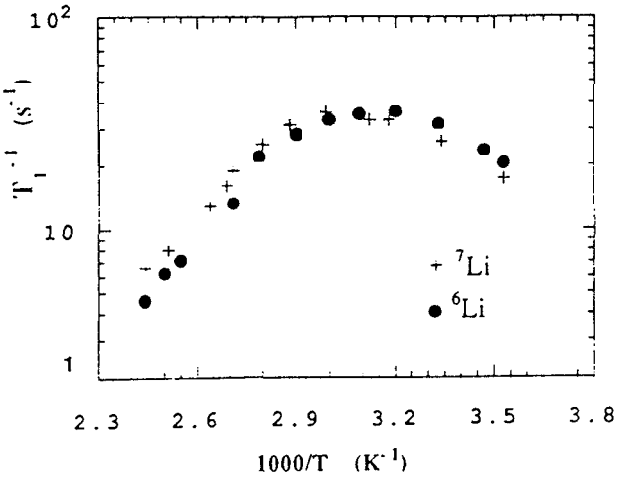

Figure 11.: Comparision between the relaxation rates $1/T_1$ of protons in P(EO) $(LiClO_4)_{0.125}$ complex with 100% of ^{6}Li (o) and 100% of ^{7}Li (+) in a cooling process for 28511' < T < $400K$. The resonance frequency was $\nu_0 = 19$MHz.

on the relaxation rates of ^{7}Li and 'H in the polymer chains. Thus, the observed ^{7}Li nuclei relaxation rates are principally due to quadrupolar relaxation induced by molecular reorientations and to inodulation of magnetic dipolar interactions between ^{7}Li nuclei. The relative contributions of these two mechanisms will be the subject of further studies. For the chain segments, these results show that the 'H relaxation is essentialy induced by the modulation of the proton-proton dipolar interactions.

A study of lithium relaxation time in the laboratory frame performed in poly(propylene-glycol) complexed with $LiCF_3SO_3$ [18], shows that coupling between mobile Li^S ions and structural relaxation of polymer chains are important processes to explain the cation diffusion.

III.4. Influence of the glass-temperature T_g

A typical curvature of the conductivity a versus $1/T$ can be modeled with a free-volume equation:

$$\sigma = \frac{A}{T^{1/2}} \exp \frac{-E_a}{k(T - T_0)}, \qquad (5)$$

where A is a pre-exponential term, k is the Boltzmann's constant, E_a is a pseudo-activation energy and T_0 is tlié ideal glass traiisition temperature. This model is based on the Vogel-Tammann-Fulcher (VTF) theory[21] wliich expresses the idea that a critical volume V* must be obtained from fluctuations adjacent to the mobile particles. All transport or relaxation properties, $DT^{-1/2}$ (diffusion), $\eta^{-1}T^{-1/2}$ (viscosity), $\sigma T^{-1/2}$ (conductivity) and $\epsilon T^{-1/2}$ (dielectric constant), vary as $\exp -(E_a/T - T_0)$. The validity of equation (5) has been verified in polypropylene oxide complexes (PPO-Li and $NaCF_3SO_3$) over four orders of magnitude of the conductivity. These complexes are perfectly amorphous at any temperature due to the lack of stereoregularity of the backbone (chemically blocked coiifigurational entropy). It should be noted that the so-called WLF expression (from Williams, Londel, Ferry) is more familiar to polymer scientists[22] :

$$\frac{\sigma(T)}{\sigma(T_{\rm ref})} = \exp \frac{C_1(T - T_{\rm ref})}{C_2 + T - T_{\rm ref}}, \qquad (6)$$

This expression, excepted for the $T^{1/2}$ term, is identical to the VTF ones if we take C_1C_2 = E, and $C_2 = T_{\rm ref} - T_0$. $T_{\rm ref}$ can be chosen as the experimentally accessible T_g. Less empirical approaches were also proposed in references[23,24]. These provide a better explanation of the motion mechanism at microscopic level. Diffusion in partially disordered matter is an important phenomenon both in practice and theory and deserves further attention.

In the systems $P(EO)(LiClO_4)_x$ the spin-lattice relaxation rates of various nuclei can be superimposed on a reduced temperature scale, independent of the salt content. We show in Figure 12 the lithium and proton spin-lattice relaxation rates as a function of inverse temperature $1/(T - T_g)$ for the composition $x = 0.166, 0.126$ and 0.222. The glass transition temperatures were obtained for each concentration from differential scanning calorimetry data. It is clear that tlie reorganization of chains is an important parameter for relaxation of nuclei. As previously demonstrated, ^{7}Li motions are closely related to segmenta1 movement of chains for all salt concentrations.

Killis et al[25] obtained the same results by studying ^{7}Li linewidth versus temperature in polyether-polyurethane network containing lithium perchlorate. They suggest that the elementary processes involved in ionic conduction and deduced from NMR data on dissolved cations reflect essentially the same phenomenon. Both results can be described within a free-volume framework characterized by the same thermal expansion factors.

III.5. Diffusion coefficient

Diffusion is another important process associated with conductivity. In electrochemistry, the identification of the contribution of differents species, and the determination of their transport and transference numbers are required. One possibility to obtain them is to use a pulsed magnetic field gradient method (PMFG) a technique introduced by Stejskal and Tanner[26]. The PMFG inetliod differs from the well-known tracer technique in several points mhich are developed in ref. [13]. An important one is that this technique is nondestriictive and can be repeated on the same sample, for iiistarice, at differeiit temperatures. The diffusion constant can be evaluated from the spin-echo decay of the NMR signal by applying a known magnetic field gradient. It is possible to measure quite accurately diffusion

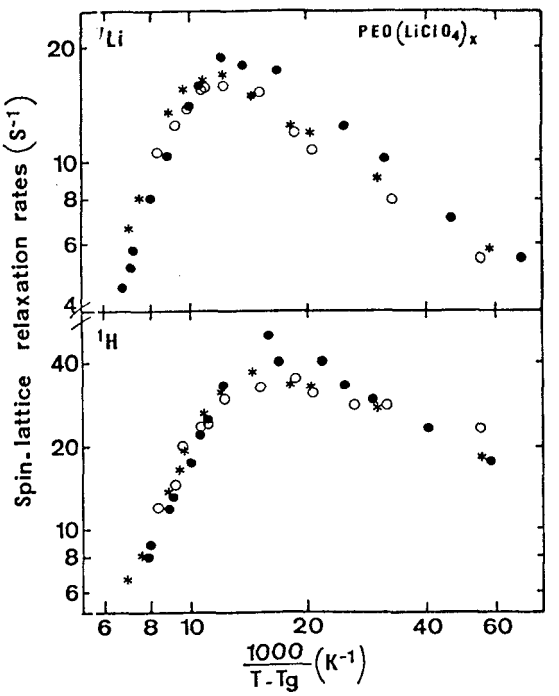

Figure 12.: Lithium and proton spin-lattice relaxation rates as a function of $1/(T - T_g)$ at the Larmor frequency of 19 MHz in P(EO) $(LiClO_4)_x$ for the comparision x = 0.125 (•); x = 0.166 (*) and x = 0.222 (o).

coefficients in the range $10^{-9} - 10^{-5}$ cm²/s, provided that the spin-spin relaxation time T_2 is not too small ($> 100\mu s$).

To treat the data, we have to assume that the nucleus under investigation has a translational random motion which is correctly described by the usual diffusion equation: $\delta n/\delta t = -D\Delta n$ where n is the number of ions per unit volume. In the system $P(EO)(M^+X^-)_x$, the cationic and anionic diffusion coefficients have approximately the same temperature dependence[27] and diffusional processes seem to have identical nature. It is interesting to observe that in most complexes, anions are more mobile (in terms of diffusion coefficient) than cations. The fact that cations and not anions interact with the chain must be emphasized. However, a similar inequality in terms of diffusion coeficients is also observed for solution of salts in dipolar liquids, and this points towards a common mechanism.

Deviations are however observed in $P(EO)(LiCF_3SO_3)_x$; they can be interpreted in term of pairs or multiplet-ions[28]. Species like $[Li(CF_3SO_3)_2]^-$ are formed from the association of a $CF_3SO_3^-$ ion and a $Li(CF_3SO_3)$ ion pair and are subject to translation diffusion, where the nuclei ^7Li and ^{19}F appear coupled[29]. Their motion will contribute to an apparent diffusion coefficient.

111.6. Transport number

Cationic and anionic transport numbers t^* are defined as the ratio a = u* la between cationic or anionic conductivity $\sigma^\pm$ and the total conductivity. By application of the Nernst-Einstein equation, $a = Ne^2(D^+ + D^-)/kT$, where N is the number of carriers/cm³ (taking $N^+ = N^-$) and $D^\pm$ are the cationic and anionic diffusion coefficients, we deduce that $t^\pm = D^\pm/(D^+ + D^-)$.

In P(EO) complexes, t^+ is such that: $0.2 < t^+ < 0.4$. Theoretically, we have to consider that the salt is completely dissociated and the calculation must be made with the total number of particules (ionized and ion pairs). The Fuoss theory[29] predicts a majority of ion pairs or triplets in solvents of low dielectric constant similar to that of PEO ($\epsilon \approx 5$). However, there are strong indications that the large entropy factor for solvation in polyethers[30,31] is favorable to an appreciable ionic dissociation. If these findings are corroborated, solvated polymers would at this point differ from conventional liquids. Salts of heavier alkali metals (K, Cs) seem to be completely dissociated, but for more polarizing Li^+, there is a marked dependence with the type of counter charge. For instance the Nernst-Einstein equation is obeyed for $LiClO_4$, but as mentioned above, not for $LiCF_3SO_3$ [27].

An interesting experimental possibility for determining the percentage of dissociated ions is to perform pulsed magnetic field gradient spin-echo experiment with the application of a pulsed electric potential gradient[32]. This method has been used to determine simultaneously the ionic mobility u^+, the transport number t^+ and the self diffusion coefficient D^+ in liquid electrolytic solutions. Neutral species, in particular, are insensitive to the application of an electric field. The only other technique giving access to mobility and not to the concentration mobility product is the Hall effect; however, its application to slow ionic particles with mobilities $\approx 10^{+7}$ times smaller than that of the electron, is extremely difficult.

IV. Conclusions

NMR techniques have proved in the last years to be a powerful tool in the study of ionic conductors. They are well adapted to the study of new materials presenting high ionic mobility and to the identification of mobile species, thus can also provide information on the structural aspect of the atorns. In solid polymer electrolytes, NMR mainly provides detailed information on the dynamics of polymer and mobile ions, such as the activation energies, the correlation times and a direct determination of the macroscopic diffusion coefficients.

Although this overview of NMR investigations in P(EO) complexes is not exhaustive, we hope that it gives an idea of the many possibilities of this technique. The recent progress in the understanding of conduction

mechanisms in polymers comes, for an appreciable part, from NMR experiments. Further refinement is not limited by the technique itself, but by how reproducible "soft matter" like organic macromolecules can be. The influence of thermal and mechanical history, in addition to the more accessible parameters like purity or molecular weight distribution, is important and should be assessed. On the other hand, the possibilities offered to taylor the polymer architecture towards new materials are infinite and this field will continue to motivate the scientific community and NMR techniques will undoubtelly help to understand better their properties.

References

1. For general reviews and references, see Polymer Electrolytes Reviews I & II, J. R. MacCallum and C. A. Vincent eds. Elsevier Applied Science, London (1989); M. Arinand, Angewandte Chemie-Advanced Materials (1990).
2. Y. Chatani and S. Okamura Polymer 28, 1815 (1987).
3. C. Berthier, W. Gorecki, M. Minier, M. B. Armand, J. M. Chabagno and P. Rigaud, Solid State Ionics **11**, 91 (1983).
4. M. Minier, C. Berthier and W. Gorecki, J. Physique 45, 739 (1984).
5. W. Gorecki, R. Andreani, C. Berthier, M. B. Armand, M. Mali, J. Ross and D. Brinkmann, Solid State Ionics **18-19**, 295 (1986).
6. A. Abragam *Principles* of Nuclear Magnetism (Oxford Press, U.K., 1978), pg 111.
7. Y. Takahashi and H. Tadokoro, Macromolécules 6, 672 (1973).
8. P. Donoso, T. J. Bonagamba, H. Panepucci, L. N. Oliveira, W. Gorecki, C. Berthier and M. Armand, to be publislied.
9. E. C. Reynhardt and J. A. Lourens, J. Chem. Phys. 80, 6240 (1984) and H. Lecavelier, F. Devreux, M. Nechtschein and G. Bidan, Mol. Cryst. Liq. Cryst. 118, 183 (1985).
10. G. R. Miller and H. S. Gutowsky, J. Chem. Phys. **39,** 1983 (1963).
11. M. C. Wintergill, J. J. Fontanella, J. P. Calame, M. K. Smith, T. B. Jones, S. G. Greenbaum, K. J. Adamic, A. N. Shetty and C. G. Audeen, Solid State Ionics **18-19**, 326 (1986).
12. N. Bloembergen, E. M. Purcell and R. V. Pound, Phys. Rev. 73 , 679 (1348).
13. D. Brinkmann, Magnetic Resonance Review 14, 101 (1985).
14. C. A. Sholl, J. Phys. C: Solid State Phys. **14**, 447 (1981).
15. E. Fukushima and S. B. W. Roeder, Experimental pulse NMR, (Addison-Wesley, London, 1981).
16. P. Donoso, W. Gorecki, C. Berthier, F. Defendini, C. Poinsignon and M. B. Armand, Solid State Ionics 28-30, 969 (1988).
17. M. A. Ratner, Polymer Electrolyte Reviews I (ref [1]).
18. S. M. Chung, K. R. Jeffrey and J. R. Stevens, J. Chem. Phys. 94, 1803 (1991).
19. R. Blinc and D. C. Ailion, B. Gunther and S. Zumer, Phys. Rev. Letters 57, 2826 (1986).
20. M. Villa and J. L, Bjorkstam, Solid State Ionics 9-10, 1421 (1983).
21. G. S. Fulcher, J. Am. Ceram. Soc. **8,** 339 (1925).
22. M. F. Williains, R. F. Landel and J. D. Ferry, J. Am. Chem. Soc. 77, 3701 (1955).
23. S. D. Druger, M. A. Ratner and A. Nitzan, Solid State Ionics 9-10, 1115 (1983).
24. T. Miyamoto and K. Shibamaye, J. Appl. Phys. 44 5372 (1973).
25. A. Killis, J. F. Le Nest, A. Gandini and H. Cheradame, Polymer Bull. **6,** 351 (1982).
26. E. O. Stejskal and J. E. Tanner, J. Chem. Phys. 42, 288 (1965).
27. W. Gorecki, P. Donoso, C. Berthier, M. Mali, J. Roos, D. Brinkmann and M. B. Armand, Solid State Ionics 28-30, 1018 (1988).
28. S. Bhattacharja, S. W. Smoot and D. H. Whitmore, Solid State Ionics **18-19**, 306 (1986).
29. C. A. Vincent, *Progress in* Solid State *Chemistry*, 17, 145. G. M. Rosenblatt and W. L. Worrel. Eds. (Pergamon Press, Oxford, 1987).
30. J. R. Stevens and P. Jacobsson, Can. J. Chem. 69, 1980 (1991).
31. S. Takeoka, K. Horiuchi and E. Tsuchida, Solid State Ionics 50, 175 (1992).
32. M. Holz, O. Liicas and C. Müller, Journal of Magn. Res. 58, 294 (1984).
33. P. A. Beckmann, Phys. Rep. **171**, 85 (1988).